

Research Paper

Method for Calculating the Sound Absorption Coefficient
for a Variable Range of Incidence Angles

Alfio YORI

*Austral University of Chile
Faculty of Engineering Sciences
Institute of Acoustics*

General Lagos 2086, Valdivia, Chile; e-mail: ayori@uach.cl

(received June 7, 2019; accepted October 10, 2019)

The theoretical estimation of sound absorption coefficient of a surface may give very different results. This will depend on the type of sound field assumed in the theoretical model used for the estimation of its sound absorption coefficient. Absorption coefficients for normal and diffuse sound fields are widely known, although they may be far from the absorption values given by an absorbing material when it is finally installed inside a room or enclosed space, where a sound field closer to a spherical wavefront is more likely to be found. This work presents a theoretical study, which is addressed at obtaining a mathematical expression to calculate the sound absorption coefficient for a variable range of incidence angles, called α_s . The presented method uses a circular sound field incidence as an approximation to a spherical incidence. The estimation of this coefficient α_s is based on obtaining the incident and reflected sound fields for a surface located facing a lineal source. The advantage of this calculation method over others lies on its capability to give results for circular, normal and random wave incidence depending on the range of incidence angles considered in the calculation.

Keywords: sound absorbing material; sound absorption coefficient; circular wave incidence.

1. Introduction

The different methods to obtain the absorption coefficient may be classified depending on the acoustic surrounding required to carry out the measurement. These may be divided into three groups: (i) impedance tube (ISO10534-2, 1996; ISO10534-1, 2000; PUTRA *et al.*, 2015), (ii) reverberation room (ISO354, 1985; MIKULSKI, 2013), and (iii) free field (MOMMERTZ, 1995; GARAI, 1993; YUZAWA, 1975; NOCKE, 2000; PLEBAN, 2013).

When a sound absorbing material is used under real conditions, the sound field it will be exposed to will depend on factors such as the size of the absorbing material or the distance between the sound source and the material. These two factors will determine the angle interval with which the wavefront components will impinge over the absorbing surface. The main estimation or measurement methods for the sound absorption coefficient assume either a normal incidence sound field or a random incidence sound field over the sample. Outside laboratory conditions, it is little probable to find a sound field completely diffuse (ISO354,

1985) or one composed by a plane wavefront impinging in a normal direction on the sample to be measured (ISO10534-2, 1996; ISO10534-1, 2000). This is why it is considered that a sound field closer to spherical wavefront better approximates to the one that would be found in a real situation inside an enclosed space. First, if we compare it to the plane wavefront assumed in the impedance tube method, in a spherical wavefront the wave will impinge on the sample with different angles and not with only one as is the case of the impedance tube. This way, the measurement will give an absorption coefficient assessed on an interval of angles and not only at normal incidence. In the method of the reverberation room, where a completely diffuse sound field is assumed, all the possible incidence angles are considered to obtain the sound absorption. Instead, if a spherical wavefront is considered, the interval of angles with which the wavefront impinges over the sample will be a function of both the distance from the source to the sample and the sample longitude as well (see Fig. 1); important factors if dimensions existing inside an enclosed space are considered.

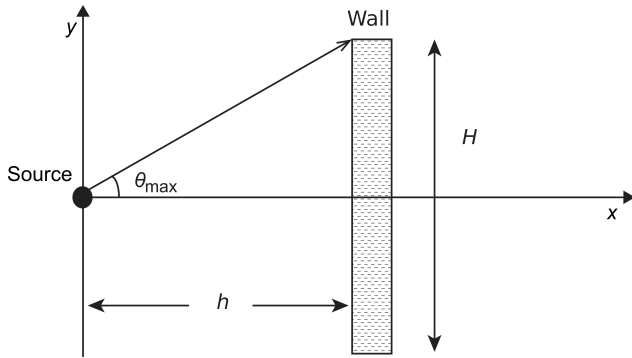


Fig. 1. Maximum angle of incidence for a wall of length H , in front of a point source at a distance h .

In this work a circular sound field incidence is used as an approximation to a spherical incidence. Although, under real conditions, the sound field impinging on a wall tends to a spherical sound field; a circular incidence, which is the two-dimensional case of the former, will not only provide a good approximation, but will also allow varying the range of incidence angles.

Thus, a sound absorption coefficient for a variable range of incidence angles is obtained in this work. This estimation allows defining an incidence interval angle to obtain a theoretical sound absorption coefficient that better represents the absorption value presented by the sample under real conditions. This absorption coefficient α_s will provide the same result as that presented by the method of normal incidence estimation or by the method of diffuse incidence estimation, depending on the incidence interval angles considered.

2. Line source in front of a plane. Obtaining the sound field

The sound field radiated over the plane (x, y) by a line source located along the z axis, without any variation of pressure amplitude along the z axis, may be represented as a sum of plane waves, where each one of them is emitted with a determined radiation angle (see Fig. 2), through the expression (MÖSER, 1988; 2009; O'NEIL *et al.*, 2014; WILLIAMS, 1999; FAHY, 2001)

$$\begin{aligned} p_i &= \frac{1}{2\pi} \int_{-\infty}^{\infty} P(k, x) e^{jk_y y} dk \\ &= \frac{\rho_0 c}{2\pi} \int_{-\infty}^{\infty} \frac{k_0}{k_r} e^{-jk_r x} e^{jk_y y} dk, \end{aligned} \quad (1)$$

where $P(k, x)$ represents the complex amplitudes of the spatial harmonic components with spatial frequency or wavenumber equal to variable k ; c is the sound velocity and ρ_0 is the volumetric density. Furthermore, this sound field may be represented directly as a point source located in the origin of the plane

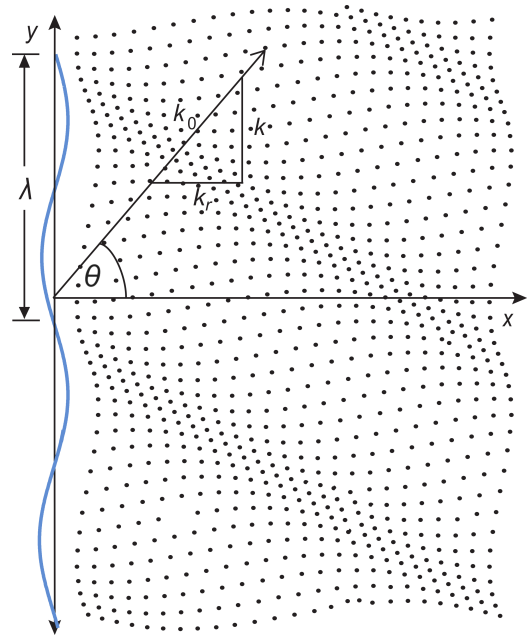


Fig. 2. Monochromatic radiator with $k = 2\pi/\lambda$.

(x, y) , without any variation of the velocity amplitude in direction of the axis z , producing circular waves (MÖSER, 1988)

$$p_i = \frac{1}{2} \rho_0 c k_0 H_0^{(2)}(k_0 \sqrt{x^2 + y^2}), \quad (2)$$

where $H_0^{(2)}$ denotes a Hankel function, second type and order zero. A sound pressure field generated by a point source located in origin is shown in Fig. 3. This figure shows that the propagation direction of each one of these components is given by the wave vector $\mathbf{k}_0 = (k_r, k)$, where $k_r = k_0 \cos \theta$ and $k = -k_0 \sin \theta$, being θ the angle respect to the axis x , with which the plane wave is propagated, which changes as k takes different values in the integral given by the Eq. (1).

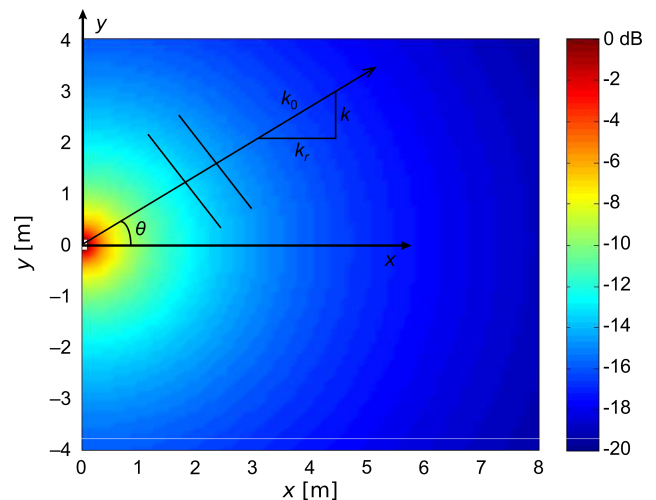


Fig. 3. Sound field produced by a point source.

Thus, for $0 \leq |k| < k_0$, we have that $k_r = \sqrt{k_0^2 - k^2}$ and the propagation angle of the plane wave is real, varying between $\theta = 0^\circ$ and $\theta = 90^\circ$. For $|k| > k_0$, k_r is imaginary and the wave is propagated along the axis y as an evanescent wave, whose amplitude exponentially decreases towards the axis x . Here, $k_r = -j\sqrt{k^2 - k_0^2} = -jk'_r$, where k'_r tends ∞ as k increases, producing that the pressure p_i corresponding to these components tends to zero. Hence, the sound pressure expression for this type of wave results

$$p_i = \frac{\rho_0 c}{2\pi} \int_{-\infty}^{\infty} j \frac{k_0}{k'_r} e^{-k'_r x} e^{jk_y} dk. \quad (3)$$

An example of evanescent wave propagating along the axis y and decaying in amplitude in the x direction is shown in Fig. 4.

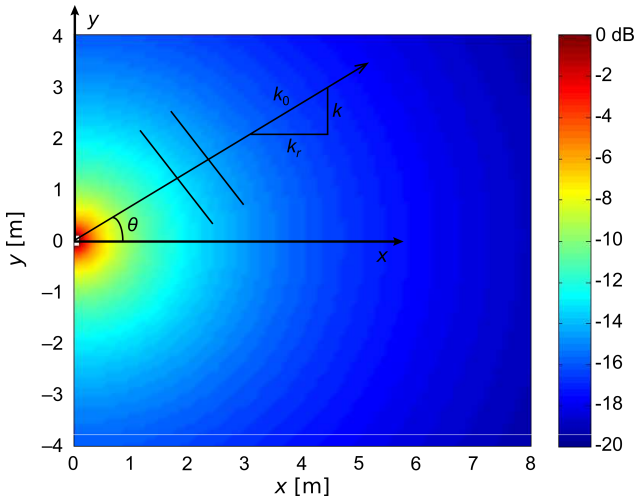


Fig. 4. Evanescent wave or near field component.

Now, if a plane surface possessing impedance z is located in front of the line source and over the plane $x = h$, as see in Fig. 5, Then, starting from the incident sound pressure p_i given by the Eq. (1), the sound pressure reflected from the interface is defined as

$$p_r = \frac{\rho_0 c}{2\pi} \int_{-\infty}^{\infty} R_p(k) \frac{k_0}{k_r} e^{jk_r x} e^{jk_y} dk, \quad (4)$$

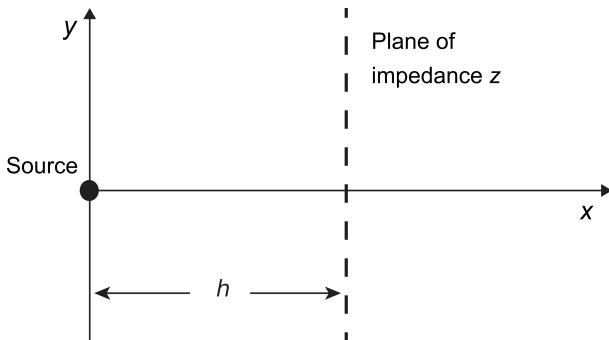


Fig. 5. Impedance plane in front of a point source.

an expression representing the reflected sound field as a sum of an infinite components number of plane waves, being $R_p(k)$ the sound reflection coefficient given by the surface for each one of the components of the incident wave.

Then, the incident sound field plus the reflected sound field has the form

$$p = p_i + p_r = \frac{\rho_0 c}{2\pi} \int_{-\infty}^{\infty} \frac{k_0}{k_r} [e^{-jk_r x} + R_p(k) e^{jk_r x}] e^{jk_y} dk. \quad (5)$$

In the plane $x = h$ where the surface is located, the conditions of sound pressure continuity p and normal velocity v_x must be accomplished; which permits to obtain the expression of the wall superficial impedance z , given by

$$z = \left(\frac{p}{v_x} \right)_{x=h}. \quad (6)$$

Now, from

$$v_x = \frac{j}{\omega \rho_0} \frac{\partial p}{\partial x} \quad (7)$$

or

$$v_x = \frac{1}{2\pi} \int_{-\infty}^{\infty} [e^{-jk_r x} - R_p(k) e^{jk_r x}] e^{jk_y} dk \quad (8)$$

and

$$p - z v_x = 0, \quad (9)$$

we have that in $x = h$

$$R_p(k) e^{jk_r h} \left(\frac{k_0}{k_r} + \frac{z}{\rho_0 c} \right) = \frac{z}{\rho_0 c} e^{-jk_r h} - \frac{k_0}{k_r} e^{-jk_r h}. \quad (10)$$

Thus, the wall z impedance is equal to

$$z = \rho_0 c \frac{k_0}{k_r} \left[\frac{1 + R_p(k) e^{j2k_r h}}{1 - R_p(k) e^{j2k_r h}} \right] \quad (11)$$

and

$$R_p(k) = e^{-j2k_r h} \left[\frac{\frac{z}{\rho_0 c} \frac{k_r}{k_0} - 1}{\frac{z}{\rho_0 c} \frac{k_r}{k_0} + 1} \right]. \quad (12)$$

This way, the sound pressure reflected from the surface located in $x = h$ takes the form

$$p_r = \frac{\rho_0 c}{2\pi} \int_{-\infty}^{\infty} \frac{k_0}{k_r} \left[\frac{\frac{z}{\rho_0 c} \frac{k_r}{k_0} - 1}{\frac{z}{\rho_0 c} \frac{k_r}{k_0} + 1} \right] e^{jk_r(x-2h)} e^{jk_y} dk, \quad (13)$$

and by symmetry with the axis x , it is reduced to

$$p_r = \frac{\rho_0 c}{\pi} \int_0^{\infty} \frac{k_0}{k_r} \left[\frac{\frac{z}{\rho_0 c} \frac{k_r}{k_0} - 1}{\frac{z}{\rho_0 c} \frac{k_r}{k_0} + 1} \right] e^{jk_r(x-2h)} \cos(ky) dk. \quad (14)$$

Now, the Eq. (14) may be separated into two integration intervals. The interval I_1 for the $k < k_0$ considering only the far field components or propagated waves of the reflected field; and the second one I_2 for the $k > k_0$ considering the near field components or

evanescent waves, which are only propagated on the reflecting surface parallel to it. Hence

$$p_r = \rho_0 c k_0 [I_1 + I_2] \quad (15)$$

with

$$I_1 = \frac{1}{\pi} \int_0^{k_0} \frac{1}{k_r} \left[\frac{\frac{z}{\rho_0 c} \frac{k_r}{k_0} - 1}{\frac{z}{\rho_0 c} \frac{k_r}{k_0} + 1} \right] e^{jk_r(x-2h)} \cos(ky) dk \quad (16)$$

and

$$I_2 = \frac{1}{\pi} \int_{k_0}^{\infty} \frac{1}{k_r} \left[\frac{\frac{z}{\rho_0 c} \frac{k_r}{k_0} - 1}{\frac{z}{\rho_0 c} \frac{k_r}{k_0} + 1} \right] e^{jk_r(x-2h)} \cos(ky) dk. \quad (17)$$

a) Integral I_1 ($k < k_0$). To develop this first integral, the following substitution is carried out

$$\begin{aligned} k &= k_0 \sin \theta, \\ dk &= k_0 \cos \theta d\theta, \\ k_r &= \sqrt{k_0^2 - k^2} \sin^2 \theta = k_0 \cos \theta, \\ \frac{dk}{k_r} &= d\theta, \end{aligned}$$

thus

$$I_1 = \frac{1}{\pi} \int_0^{\pi/2} \left[\frac{\frac{z}{\rho_0 c} \cos \theta - 1}{\frac{z}{\rho_0 c} \cos \theta + 1} \right] \cdot e^{jk_0 \cos \theta(x-2h)} \cos(k_0 y \sin \theta) d\theta \quad (18)$$

an expression which gives the plane wave components of the reflected sound field possessing a propagation angle between 0 and $\pi/2$.

b) Integral I_2 ($k > k_0$). Evanescent waves are also known as subsonic waves as they travel at a velocity lower than that used by sound in the air. Therefore, the wave number component k_r of this type of waves is imaginary. Although these waves travel parallel to the surface holding them, they are assumed to possess a complex propagation angle (FRISK, 1979)

$$\theta = \pi/2 - ju. \quad (19)$$

This way, as

$$\sin \theta = \sin[\pi/2] \cosh[u] - j \cos[\pi/2] \sinh[u], \quad (20)$$

then we have that

$$\sin \theta = \cosh u. \quad (21)$$

This way, for the development of this integral the following substitution is used

$$k = k_0 \cosh u \quad (22)$$

from which one obtains

$$\begin{aligned} dk &= k_0 \sinh u du, \\ k_r &= -j \sqrt{k^2 - k_0^2}, \\ k_r &= -jk_0 \sqrt{\cosh^2 u - 1}, \\ k_r &= -jk_0 \sinh u, \end{aligned}$$

and

$$\begin{aligned} \frac{dk}{k_r} &= \frac{du}{-j} = j du, \\ \frac{k_r}{k_0} &= -j \sinh u, \end{aligned}$$

resulting

$$I_2 = \frac{j}{\pi} \int_0^{\infty} \left[\frac{\frac{jz}{\rho_0 c} \sinh u + 1}{\frac{jz}{\rho_0 c} \sinh u - 1} \right] \cdot e^{k_0 \sinh u(x-2h)} \cos(k_0 y \cosh u) du \quad (23)$$

an expression providing the contribution given by the near field components to the total reflected field p_r .

The sound field given by the Eq. (14) may be interpreted as generated from an image source, symmetrically located with the reflecting surface and the real point source. Now, the sound field reflected from the surface will behave as if coming from a virtual point source only if the wall impedance $z = \infty$ and both integrals are considered; that is, both the near field I_2 and the far field I_1 as well. Figure 6 shows the incident sound pressure p_i produced by a point source such as the one shown in Fig. 5, on a surface located at a distance $h = 3$ from the source. Now, if the reflecting surface presents a superficial impedance $z = 100\rho_0 c$, then,

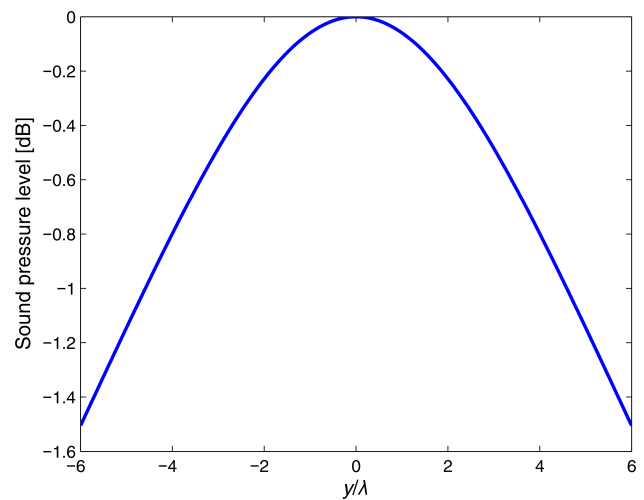


Fig. 6. Level of incident sound pressure $|p_i|$ produced by a point source over a surface located at a distance $h = 3$ from the source; $f = 680$ Hz.

the virtual point source must produce the same sound pressure distribution on the plane where the surface is located, that is $p_i = p_r$ in the plane $x = 3$. Figure 7 shows the reflected sound pressure distribution p_r composed only by the far field I_1 given by the Eq. (18). Figure 8 shows the reflected sound field p_r , this time adding the near field I_2 given by the Eq. (23), for different intervals of the integration variable u .

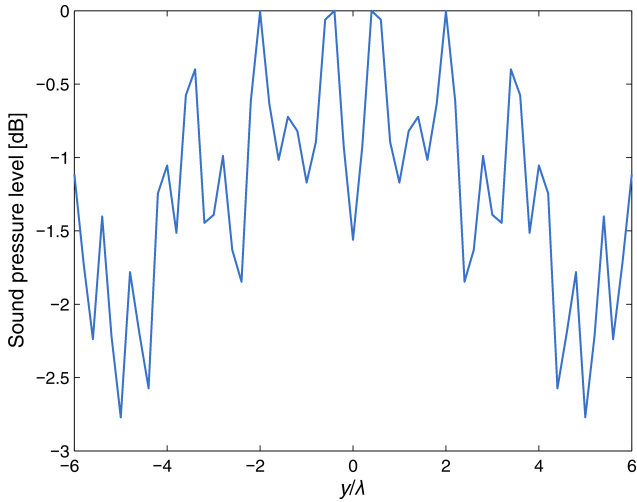


Fig. 7. Level of reflected sound pressure $|p_r|$ composed only by the far field components I_1 , on the plane of a surface of impedance $z = 100\rho_0c$, located at a distance $h = 3$ from the source; $f = 680$ Hz.

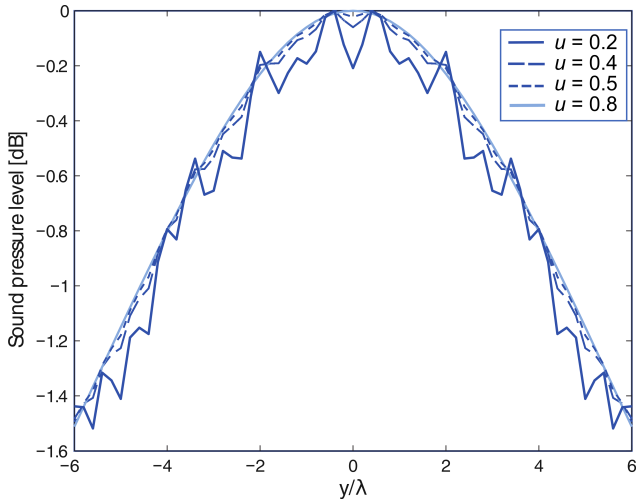


Fig. 8. Level of reflected sound pressure $|p_r|$ composed by the far field I_1 and the near field I_2 , on the plane of a surface of impedance $z = 100\rho_0c$, varying the interval of the integration variable u . Distance $h = 3$ and $f = 680$ Hz.

Figures 9, 10, and 11 respectively show the total sound field $p = p_i + p_r$ for the cases of a surface of superficial impedance $z = \rho_0c$, $z = 100\rho_0c$ and $z = -jZ_\infty \cot(k_a d)$, where d is the thickness of the absorbing material, Z_∞ its characteristic impedance

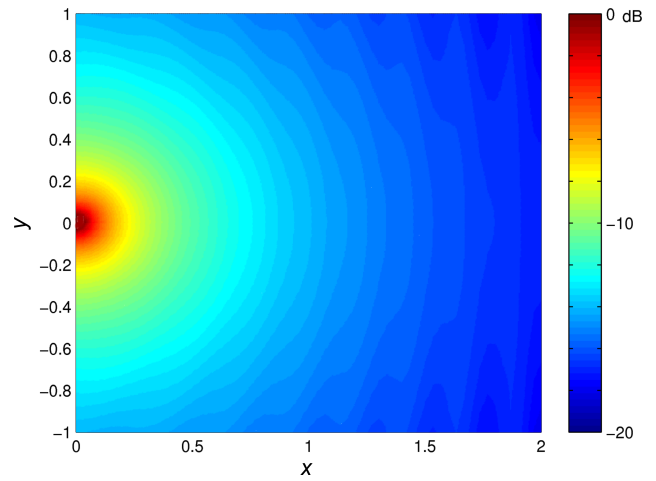


Fig. 9. Sound pressure level $|p| = |p_i + p_r|$ in front of a wall of impedance $z = \rho_0c$; $f = 800$ Hz.

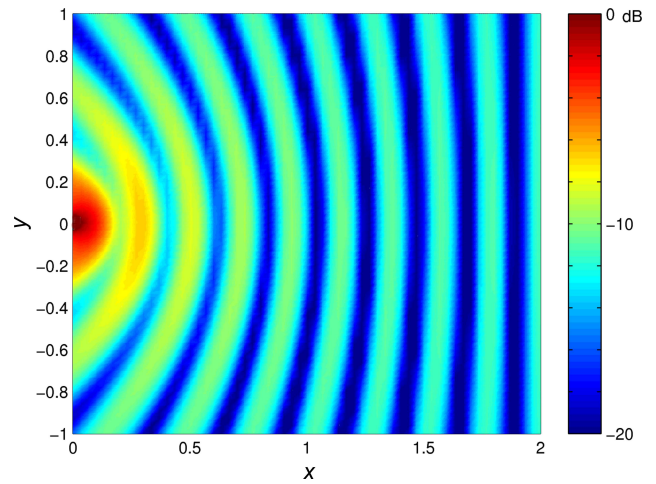


Fig. 10. Sound pressure level $|p| = |p_i + p_r|$ in front of a wall of impedance $z = 100\rho_0c$; $f = 800$ Hz.

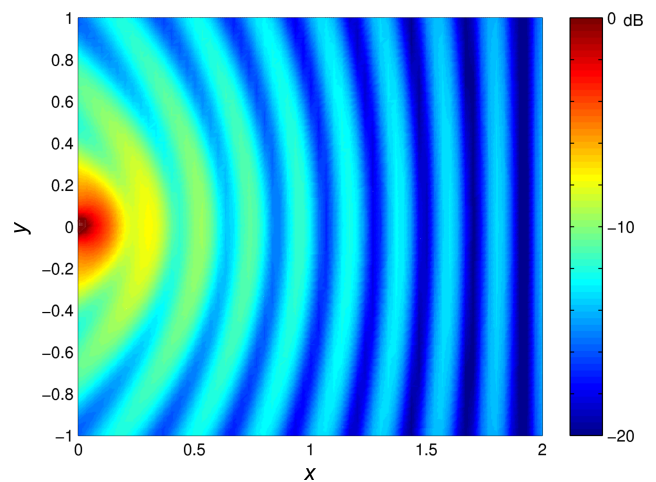


Fig. 11. Sound pressure level $|p| = |p_i + p_r|$ in front of a wall of impedance $z = -jZ_\infty \cot(k_a d)$ with normalized flow resistance $\Xi d/\rho_0c = 6.25$, $\sigma = 1$, $\kappa = 1.7$ and thickness $d = 10$ cm; $f = 800$ Hz.

which depends on the sample parameters of specific flow resistance Ξ , porosity σ and structure factor κ , and is given by MÖSER (2009)

$$Z_\infty = \rho_0 c \frac{\sqrt{\kappa}}{\sigma} \sqrt{1 - j \frac{\Xi \sigma}{w \rho_0 \kappa}}, \quad (24)$$

and k_a is the wave propagation constant inside the sound absorbing material MÖSER (2009)

$$k_a = k_0 \sqrt{\kappa} \sqrt{1 - j \frac{\Xi \sigma}{w \rho_0 \kappa}}. \quad (25)$$

All of them are located at a distance $h = 2$ from the source. Figure 12 shows particles velocity in front of the wall of impedance $z = 100\rho_0 c$.

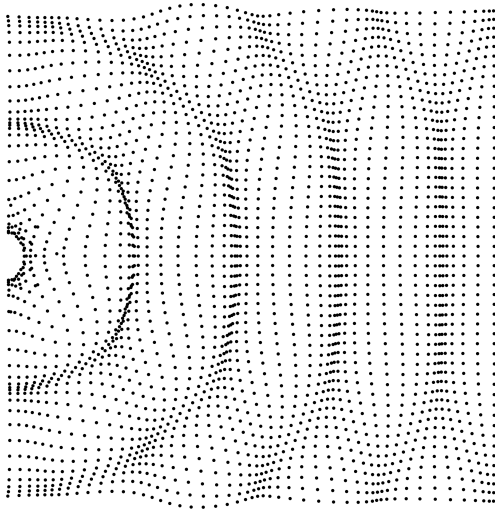


Fig. 12. Sound field in front of a surface with impedance $z = 100\rho_0 c$.

3. Sound absorption for circular sound field incidence

The sound power absorbed per unit length of a surface located in the plane $x = h$ is equal to the intensity (FAHY, 2001)

$$I_x = \frac{1}{2} \text{Re} [p(x, y) \cdot v_x^*(x, y)] \quad (\text{in } x = h) \quad (26)$$

and the total absorbed power P_α is

$$P_\alpha = \frac{1}{2} \text{Re} \left[\int_{-\infty}^{\infty} p(h, y) \cdot v_x^*(h, y) dy \right]. \quad (27)$$

From Parseval's Theorem,

$$\int_{-\infty}^{\infty} f(y) \cdot g^*(y) dy = \frac{1}{2\pi} \int_{-\infty}^{\infty} F(k) \cdot G^*(k) dk, \quad (28)$$

we have

$$P_\alpha = \frac{1}{4\pi} \text{Re} \left[\int_{-\infty}^{\infty} P(k, h) \cdot V^*(k, h) dk \right]. \quad (29)$$

Thus, from Eq. (5) and Eq. (8) we have

$$P(k, h) = \rho_0 c \frac{k_0}{k_r} [e^{-jk_r h} + R_p(k) e^{jk_r h}] \quad (30)$$

and

$$V(k, h) = e^{-jk_r h} - R_p(k) e^{jk_r h}, \quad (31)$$

then, by symmetry in k

$$P_\alpha = \frac{\rho_0 c}{2\pi} \text{Re} \left[\int_0^{\infty} \frac{k_0}{k_r} (e^{-jk_r h} + R_p(k) e^{jk_r h}) \cdot (e^{jk_r h} - R_p^*(k) e^{-jk_r h}) dk \right]. \quad (32)$$

Again, it is convenient to separate the integration interval into its components of far field and near field

$$P_{\alpha 1} = \frac{\rho_0 c}{2\pi} \text{Re} \left[\int_0^{k_0} \frac{k_0}{k_r} (e^{-jk_r h} + R_p(k) e^{jk_r h}) \cdot (e^{jk_r h} - R_p^*(k) e^{-jk_r h}) dk \right] \quad (33)$$

and

$$P_{\alpha 2} = \frac{\rho_0 c}{2\pi} \text{Re} \left[\int_{k_0}^{\infty} \frac{k_0}{k_r} (e^{-jk_r h} + R_p(k) e^{jk_r h}) \cdot (e^{jk_r h} - R_p^*(k) e^{-jk_r h}) dk \right]. \quad (34)$$

For the absorbed power $P_{\alpha 1}$, k_r takes a real value, then

$$P_{\alpha 1} = \frac{\rho_0 c}{2\pi} \int_0^{k_0} \frac{k_0}{k_r} (1 - |R_p(k)|^2) dk \quad (35)$$

and using the Eq. (12)

$$P_{\alpha 1} = \frac{\rho_0 c}{2\pi} \int_0^{k_0} \frac{k_0}{k_r} \left(1 - \left| e^{-j2hk_r} \frac{\frac{z}{\rho_0 c} \frac{k_r}{k_0} - 1}{\frac{z}{\rho_0 c} \frac{k_r}{k_0} + 1} \right|^2 \right) dk \quad (36)$$

and using substitution again, it results

$$P_{\alpha 1} = \frac{\rho_0 c}{2\pi} \int_0^{\pi/2} k_0 \left(1 - \left| e^{-j2hk_0 \cos \theta} \frac{\frac{z}{\rho_0 c} \cos \theta - 1}{\frac{z}{\rho_0 c} \cos \theta + 1} \right|^2 \right) d\theta. \quad (37)$$

On the other hand, for the absorbed power $P_{\alpha 2}$ produced by the near field, k_r takes an imaginary value $k_r = -j\sqrt{k^2 - k_0^2} = -jk'_r$. Then

$$P_{\alpha 2} = \frac{\rho_0 c}{2\pi} \text{Re} \left[\int_{k_0}^{\infty} \frac{k_0}{k_r} \cdot (e^{-2k'_r h} + (R_p - R_p^*) - |R_p|^2 e^{2k'_r h}) dk \right] \quad (38)$$

and using substitution given by Eq. (22) the result is

$$P_{\alpha 2} = \frac{\rho_0 c}{2\pi} \operatorname{Re} \left[k_0 \int_0^{\infty} j e^{-2hk_0 \sinh u} + j(R_p - R_p^*) - j|R_p|^2 e^{2hk_0 \sinh u} du \right], \quad (39)$$

being real only the term given by $j(R_p - R_p^*)$. Here, the reflection coefficient R_p given by the Eq. (12) takes the following form

$$\begin{aligned} R_p(k) &= e^{-2hk_0 \sinh u} \frac{j \frac{z}{\rho_0 c} \sinh u + 1}{j \frac{z}{\rho_0 c} \sinh u - 1} \\ &= e^{-2hk_0 \sinh u} \frac{\frac{z}{\rho_0 c} \sinh u - j}{\frac{z}{\rho_0 c} \sinh u + j}, \end{aligned} \quad (40)$$

and expressing impedance z by means of its real and imaginary parts as $a + jb$

$$R_p(k) = e^{-2hk_0 \sinh u} \frac{(a + jb) \sinh u - j\rho_0 c}{(a + jb) \sinh u + j\rho_0 c}, \quad (41)$$

then,

$$R_p(k) - R_p^*(k) = e^{-2hk_0 \sinh u} \cdot \left[-j \frac{4a\rho_0 c \sinh u}{(a \sinh u)^2 + (b \sinh u + \rho_0 c)^2} \right], \quad (42)$$

finally resulting

$$P_{\alpha 2} = \frac{\rho_0 c}{2\pi} k_0 \int_0^{\infty} e^{-2hk_0 \sinh u} \cdot \left[\frac{4a\rho_0 c \sinh u}{(a \sinh u)^2 + (b \sinh u + \rho_0 c)^2} \right] du. \quad (43)$$

Now, the sound power P_{inc} impinging over the surface is simply obtained by considering a reflection coefficient $R_p = 0$ in the Eq. (35), which gives

$$P_{inc} = \frac{\rho_0 c}{2\pi} k_0 \int_0^{\frac{\pi}{2}} d\theta = \rho_0 c \frac{k_0}{4}. \quad (44)$$

Finally, sound absorption for a circular sound field is calculated through the sound absorption coefficient α_s given by

$$\alpha_s = \frac{P_{\alpha 1} + P_{\alpha 2}}{P_{inc}}, \quad (45)$$

a coefficient which, for a semi infinite surface, considers the incidence angles between 0° and 90° of all the plane wave components composing the circular wave front.

4. Sound absorption and its dependence on the type of sound field

The type of sound field impinging on a material will determine its absorption coefficient. The sound absorption of a material obtained for a circular incidence differs from that obtained for random incidence (ISO354, 1985) and normal incidence (ISO10534-2, 1996).

Figure 13 shows the sound absorption curve of a porous surface for circular incidence, together with the absorption curves for normal plane sound field incidence and random sound field incidence. The normal incidence absorption was calculated through the equation (MÖSER, 2009)

$$\alpha_\theta = \frac{4R_e(z/\rho_0 c) \cos \theta}{(1 + R_e(z/\rho_0 c) \cos \theta)^2 + (I_m(z/\rho_0 c) \cos \theta)^2} \quad (46)$$

with $\theta = 0^\circ$ and the surface impedance z given by Eq. (24) and Eq. (25).

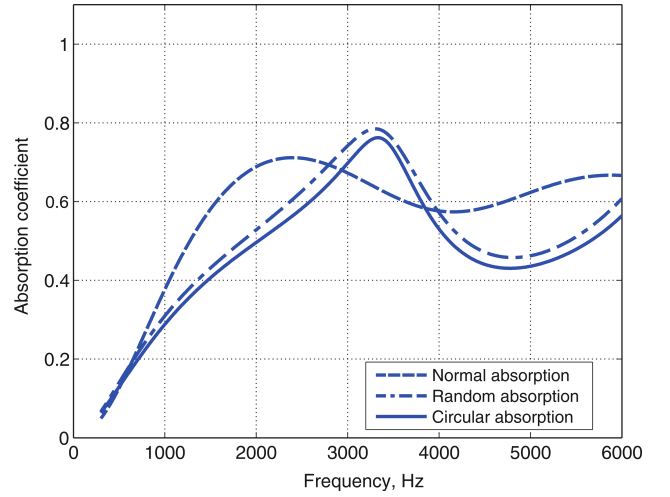


Fig. 13. Sound absorption of a semi infinite porous layer of impedance $z = -jZ_\infty \cot(k_a d)$ with normalized flow resistance $\Xi d/\rho_0 c = 0.5$, structure factor $\kappa = 1$, porosity $\sigma = 1$, and thickness d equal to 5 cm for different sound fields.

The absorption curve for random field incidence was calculated with the expression (ISO354, 1985; FAHY, 2001)

$$\alpha_r = \int_0^{\pi/2} \alpha_\theta \sin 2\theta d\theta. \quad (47)$$

Figure 13 also shows that the sound absorption curve at normal incidence for a specific material differs very much from the absorption curve at random incidence. Whereas, circular and random sound fields possess very similar sound absorption curves, though they present a constant offset between them. Both methods weight differently the sound absorption coefficients of angular incidence $\alpha(\theta)$ given by the Eq. (46). About Eq. (47), there is a limiting angle for which it is possible to consider a plane wave incidence on the sample (DEL REY *et al.*, 2014).

Figure 14 shows absorption curves of the same material for normal, random and circular sound fields; together with the curves showing the evolution of circular absorption when a range of incidence angles different from 0° to 90° is considered in its calculation. This way, the curves show that this method of calculation may give not only theoretical absorption values for a circular incidence, but also those values for normal and random incidence as well, depending on the interval of incidence angles θ considered in α_s estimation.

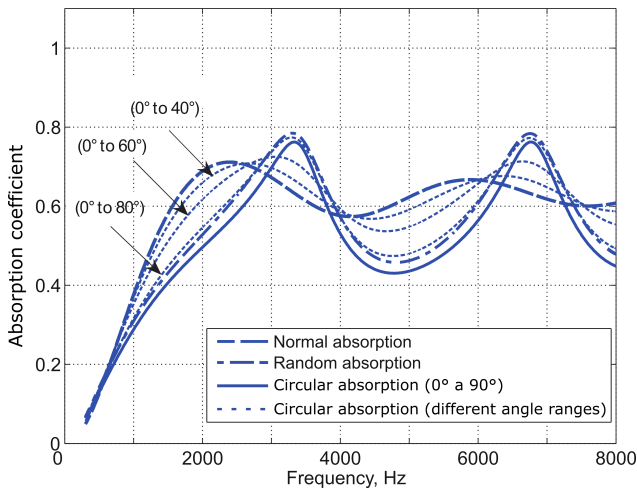


Fig. 14. Variation of α_s by varying the range of the incidence angles. Surface impedance with normalized flow resistance $\Xi d/\rho_0 c = 0.5$, structure factor $\kappa = 1$, porosity $\sigma = 1$, and thickness 5 cm, for different sound fields.

Figure 15 shows the sound absorption coefficient measured (YORI, 2015) from a foam sample with

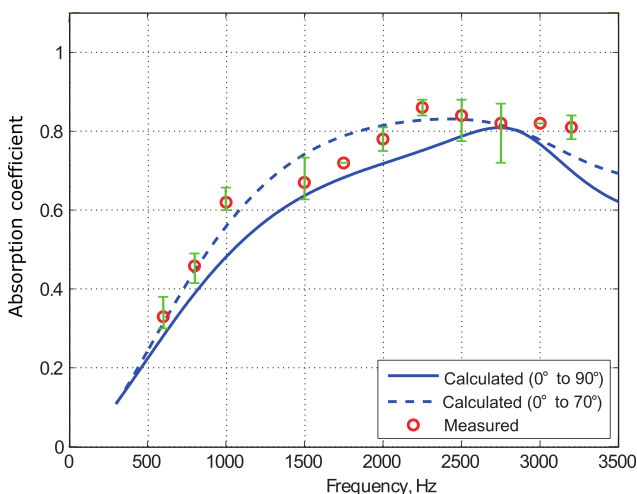


Fig. 15. Measured and calculated values of the absorption coefficient for spherical incidence. Foam with 30 kg/m^3 of density. $\Xi d/\rho_0 c = 0.875$, structure factor $\kappa = 1.4$, porosity $\sigma = 1$, and thickness 5 cm. The bar shows the difference between the highest and lowest value measured for each frequency. The mean value is shown in the curve of the measured values.

30 kg/m^3 of density and thickness 5 cm, together with the calculated values of α_s for the incidence angle ranges $\theta = 0^\circ$ to $\theta_{\text{Max}} = 90^\circ$ and $\theta = 0^\circ$ to $\theta_{\text{Max}} = 70^\circ$; the latter being the one obtained with the source position (0.4 m from the sample) and sample size used in the measurements. Four measurements were carried out. A good agreement is observed between calculated and measured values.

5. Conclusion

This theoretical model of calculation is able to deliver results for normal, random and circular incidence, only varying the range of angles of incidence considered in the calculation. The advantage of estimating sound absorption of an absorbing material using this theoretical model of circular sound field incidence instead of those highly idealized, random and normal, lies on the fact that this model allows considering variables such as distance between the sample and the source and the effective sample length. This way, this coefficient of sound absorption α_s provides a theoretical sound absorption value of a material comparatively much closer to the sound absorption given under real conditions by this material.

References

1. DEL REY R., ARENAS J.P., ALBA J., BERTÓ L. (2014), *Determination of the statical sound absorption coefficient of porous materials from normal-incidence measurements*, 21st International Congress on Sound and Vibration 2014, Beijing, China ICSV 2014, Vol. 4, pp. 3272–3279.
2. FAHY F. [Ed.] (2001), *Foundations of engineering acoustics*, Academic Press.
3. FRISK G. (1979), *Inhomogeneous waves and the plane-wave reflection coefficient*, The Journal of the Acoustical Society of America, **66**(1): 219–234, doi: 10.1121/1.383074.
4. GARAI M. (1993), *Measurement of the sound-absorption coefficient in situ: The reflection method using periodic pseudo-random sequences of maximum length*, Applied Acoustics, **39**(1–2): 119–139, doi: 10.1016/0003-682X(93)90032-2.
5. ISO 354:1985, *Acoustics. Measurements of sound absorption in a reverberation room*.
6. ISO 10534-1:1996, *Acoustics. Determination of sound absorption coefficient and impedance in impedance tubes. Part 1: Method using standing wave ratio*.
7. ISO 10534-2:1996, *Acoustics. Determination of sound absorption coefficient and impedance in impedance tubes. Part 2: Transfer-function method*.
8. MIKULSKI W. (2013), *Determining the sound absorbing coefficient of materials within the frequency range of*

- 5000–50000 Hz in a test chamber of a volume of about 2 m^3 , Archives of Acoustics, **38**(2): 177–183.
9. MOMMERTZ E. (1995), *Angle-dependent in situ measurement of reflection coefficients using a subtraction technique*, Applied Acoustics, **46**(3): 251–263, doi: 10.1016/0003-682X(95)00027-7.
 10. MÖSER M. [Ed.] (1988), *Analyse und synthese akustischer spektren*, Springer-Verlag, Berlin, Heidelberg, New York, London, Paris, Tokyo.
 11. MÖSER M., BARROS J. [Eds] (2009), *Acoustic Engineering. Theory and Applications* [in Spanish: *Ingeniería Acústica, Teoría y Aplicaciones*], 2nd ed., Springer, doi: 10.1007/978-3-642-02544-0.
 12. NOCKE C. (2000), *In situ acoustic impedance measurement using a free-field transfer function method*, Applied Acoustics, **59**(3): 253–264, doi: 10.1016/S0003-682X(99)00004-3.
 13. O’NEIL M., GREENGARD L., PATAKI A. (2014), *On the efficient representation of the half-space impedance Green’s function for the Helmholtz equation*, Wave Motion, **51**(1): 1–13, doi: 10.1016/j.wavemoti.2013.04.012.
 14. PLEBAN D. (2013), *Method of testing of sound absorption properties of materials intended for ultrasonic noise protection*, Archives of Acoustics, **38**(2): 191–195.
 15. PUTRA A., KHAIR F., NOR M. (2015), *Utilizing hollow-structured bamboo as natural sound absorber*, Archives of Acoustics, **40**(4): 601–608, doi: 10.1515/aoa-2015-0060.
 16. WILLIAMS E.G. [Ed.], (1999), *Fourier acoustics: Sound radiation and nearfield acoustical holography*, Academic Press.
 17. YORI A., MÖSER M. (2015), *A measurement method for the sound absorption coefficient for arbitrary sound fields and surfaces*, Acta Acustica united with Acustica, **101**(4): 668–674, doi: 10.3813/AAA.918862.
 18. YUZAWA M. (1975), *A method of obtaining the oblique incident sound absorption coefficient through an on-the-spot measurement*, Applied Acoustics, **8**(1): 27–41, doi: 10.1016/0003-682X(75)90004-3.